Topography of polished plates of
albite crystal and glass during dissolution

Nathan P. Mellott [1, 3], Susan L. Brantley [1,*], and Carlo G. Pantano [2]

[1] Department of Geosciences, The Pennsylvania State University, University Park, Pennsylvania 16802 USA
[2] Department of Material Science and Engineering, The Pennsylvania State University, University Park, Pennsylvania 16802 USA
[3] Present address: Department of Materials Science and Engineering, The Pennsylvania State University,
University Park, Pennsylvania, 16802

* corresponding author: brantley@geosc.psu.edu

Abstract—Polished surfaces of glass and crystal of albite composition were analyzed using atomic force microscopy (AFM) before and after dissolution at pH 2.0 and 9.0, and changes in topography were compared to dissolution rates of powders of the same phase. The roughness of the crystal plates was greater when dissolved at pH 2.0 than at pH 9.0, reflecting greater extent of etching at intrinsic crystalline and polishing defects at lower pH. In contrast, the RMS roughness of the glass plate was identical within error when dissolved at pH 2.0 and pH 9.0. The similarity in roughness of the polished glass plate as a function of pH of dissolution may be related to lack of reproducibility in polishing, different controls on dissolution for glass vs. crystalline substrates, or the presence of a thick, porous leached layer developed on the glass during dissolution at pH 2.0. The AFM only documented an increase in RMS roughness by a factor of 7 on the glass dissolved at pH 2.0 after 5000 h, while BET surface area increased by a factor of 30 on glass powder dissolved at pH 2.0 after 4000 h of dissolution. However, total roughness of the surfaces could not be quantified by AFM through analysis of only RMS roughness; spatial distribution (fractal dimension D) also had to be measured. D was calculated from the roughness exponent and from the power spectral density on several samples. These two methods of calculating D did not always yield comparable values for all samples. The surface area calculated from the RMS roughness and fractal dimension measured for several samples increased only slightly over 5000 h of dissolution at pH 2.0 for both phases, demonstrating that the AFM documented only insignificant topographic effects related to nonstoichiometric dissolution (leaching). Feldspar dissolution rates estimated from AFM measurements were within a factor of 10 of dissolution rates based upon solution results, even though rate of retreat of entire surface layers could not be quantified. Further research should continue to emphasize using AFM to document changes in roughness for comparison to dissolution measured from solution chemistry.

1. INTRODUCTION

The development of surface topography related to crystallographic features during dissolution of minerals has been noted by many workers (e.g. Helgeson et al. 1984; Brantley et al., 1986; Lasaga and Blum, 1986; Casey et al., 1988; Blum et al., 1990; White and Peterson, 1990; Anbeek, 1992; Lee and Parsons, 1995; Lee et al., 1998; Fenter et al., 2000), but quantitative measurement of the evolution of topography during dissolution is generally lacking. Instead, dissolution rates are usually related simply to the surface area as determined through gas adsorption using the Brunauer, Emmet, and Teller (BET) isotherm (Brunauer et al., 1938). The BET measurement provides total surface area accessible to the adsorbate molecule (for a review, see Brantley et al., 1999; Brantley and Mellott, 2000). New surface techniques such as scanning tunneling microscopy (STM) and atomic force microscopy (AFM) now make documentation of microscopic (μm to nm scale) to atomic (~1-5 Å) roughness possible on both conductive and nonconductive surfaces. Few comparisons have been made between changes in BET surface area of minerals during dissolution and changes in surface topography as measured by AFM.

In order to investigate the evolution of feldspar surfaces with dissolution, atomic force microscopy was used to analyze the surface topography of a unique suite of glass and crystal samples prepared by Hamilton et al. (2000). In these preparations, polished plates of albite glass and crystal (compositions summarized in Hamilton et al., 2000) were dissolved at pH 2.0 or 9.0 in batch reactors under ambient conditions far from equilibrium. Based upon comparisons of dissolved solute chemistry and thermodynamic data, Hamilton et al. (2000) concluded that secondary phases did not precipitate during dissolution. Polished plates were used so as to provide flat surfaces amenable for elemental analyses (x-ray photoelectron spectroscopy (XPS) and secondary ion mass spectrometry (SIMS)) and topographic analyses. Significant effort was expended to polish the surface with little chemical alteration.

Hamilton et al. (2000) also dissolved powders (grain size = 75-150 μm) in flow experiments at room

temperature and reported that the albite crystal and glass powders dissolved at the same rate ($\pm$ 40%) at pH 2.0 (HCl-H$_2$O) when rates were normalized by initial surface area. Error was determined by propagating uncertainties in the measurement of rates (Hamilton et al., 2000). Although the crystal and glass powders had similar initial BET surface areas (Table 1), after dissolution for 4000 h at pH 2.0, the surface areas of the glass and crystal powders increased by a factor of 30 and 2, respectively. Structures of altered, leached layers on albite crystal and glass are presumed to be more open and porous than the unaltered surface (Casey and Bunker, 1990; Hellmann, 1995, 1997; Hamilton et al., 2000), allowing proton-bearing species access deep into the near surface. However, as per the observations of Casey et al. (1989) for a different feldspar composition, Hamilton and coworkers saw no increase in dissolution rate with time for the glass dissolved at pH 2.0. They therefore interpreted the increase in specific surface area of the glass dissolved at pH 2.0 as the result of the formation of a porous leached near-surface layer. This increase in specific surface area was not thought to represent an increase in *reactive* area, and rates were thus normalized by initial surface area. Although most other researchers investigating feldspar dissolution have similarly normalized rates by initial surface area, some have normalized by final surface area (see Stillings and Brantley, 1995).

Hamilton et al. (2000) also observed that these albite crystal and glass powders dissolved in LiOH-H$_2$O at the same rate within error ($\pm$ 40%) at pH 8.4 (= outlet pH, inlet pH = 9.3). For these powder samples, BET surface areas differed minimally after dissolution for 5400 h (reacted/unreacted surface area = 1.5 for glass and 1.1 for crystal).

AFM is used here to analyze surface topography of the plates prepared by Hamilton in order to address the following questions: How does crystallinity affect RMS roughness and power spectral density of roughness during dissolution of albite? How do AFM measurements of bearing volume correlate with observed dissolution based upon solution chemistry? Can AFM-measured surface area correlate with BET surface area?

2. ANALYTICAL METHODS

2.1. Sample Preparation

Samples analyzed in this study are some of the identical plates described by Hamilton et al. (2000). Albite crystal was obtained from Wards Scientific and albite glass was prepared by melting crystalline Amelia albite and annealing it at 700 °C for ~12 hours (Zellmer,

1986; Hamilton et al., 2000). Compositions of albite crystal and glass are equal to within better than 1 wt. % for all major oxides (Hamilton et al., 2000).

Albite crystal and glass plates were cut with a diamond saw to 2 cm x 1 cm x 0.2 cm. The plates were polished to 0.1 μm using a LECO AP-60 automatic polisher in an oil-based diamond spray, followed by a final polishing to 0.05 μm with a cerium oxide/chrome oxide spray. No attempt to orient the polycrystalline samples prior to polishing was made. Based on limited observations under an optical microscope, grains of Amelia albite varied from at least a few mm to much larger in diameter. The sample preparation procedure was chosen from among many others because it provided glass and crystals with surface chemistries, as measured by x-ray photoelectron spectroscopy (XPS), that were as close as possible to the bulk stoichiometry for all elements (Hamilton et al., 2000).

Crystal plates used for this study came from batch experiments run for either 1000 or 5000 hrs (note that plates run for 5000 h were separate plates from those run for 1000 h). Glass plates were similarly reacted, but only unleached plates and plates dissolved for 5000 h were available for this study. Solutions used for dissolution experiments included: 1) trace-metal grade HCl and reverse-osmosis (RO) water at pH 2.0 2) LiOH and RO water at pH 9.0. All vessels were held at 25$\pm$1 °C in an oven and pH was constant to within $\pm$0.3 pH units. Each reaction vessel had an initial surface area to volume ratio of 5.0 x 10^{-3} cm^{-1}. Following dissolution experiments, plates were rinsed with RO water, ultrasonically cleaned in acetone, blown dry with nitrogen, and stored in a vacuum dessicator. Scanning electron microscopy (SEM) revealed no evidence for the cracking of the leached layers.

2.2. Microscopy

Plates were imaged using differential interference contrast microscopy (DIC) and a Digital Instruments Nanoscope IIIa Dimension 3100 Atomic Force Microscope before and after dissolution. Both height and amplitude images were collected in Tapping Mode®, with a sharpened tip, at a scan rate of 1.0–1.5 Hz. Multiple scans (~20) were completed on each sample at different locations on the surface. From these, three to ten representative 10 μm x 10 μm areas of each sample were then chosen for further analysis. In choosing scanning sites, cracks, grain boundaries, rip-up clasts, etc. were avoided where possible. While scanning, the cantilever records a fixed number (256) of height measurements throughout each scan line. Therefore, for a 10 μm x 10 μm scan, the lateral resolution is about 40 nm per pixel. The AFM tip also impedes resolution below approximately 10-30 nm,
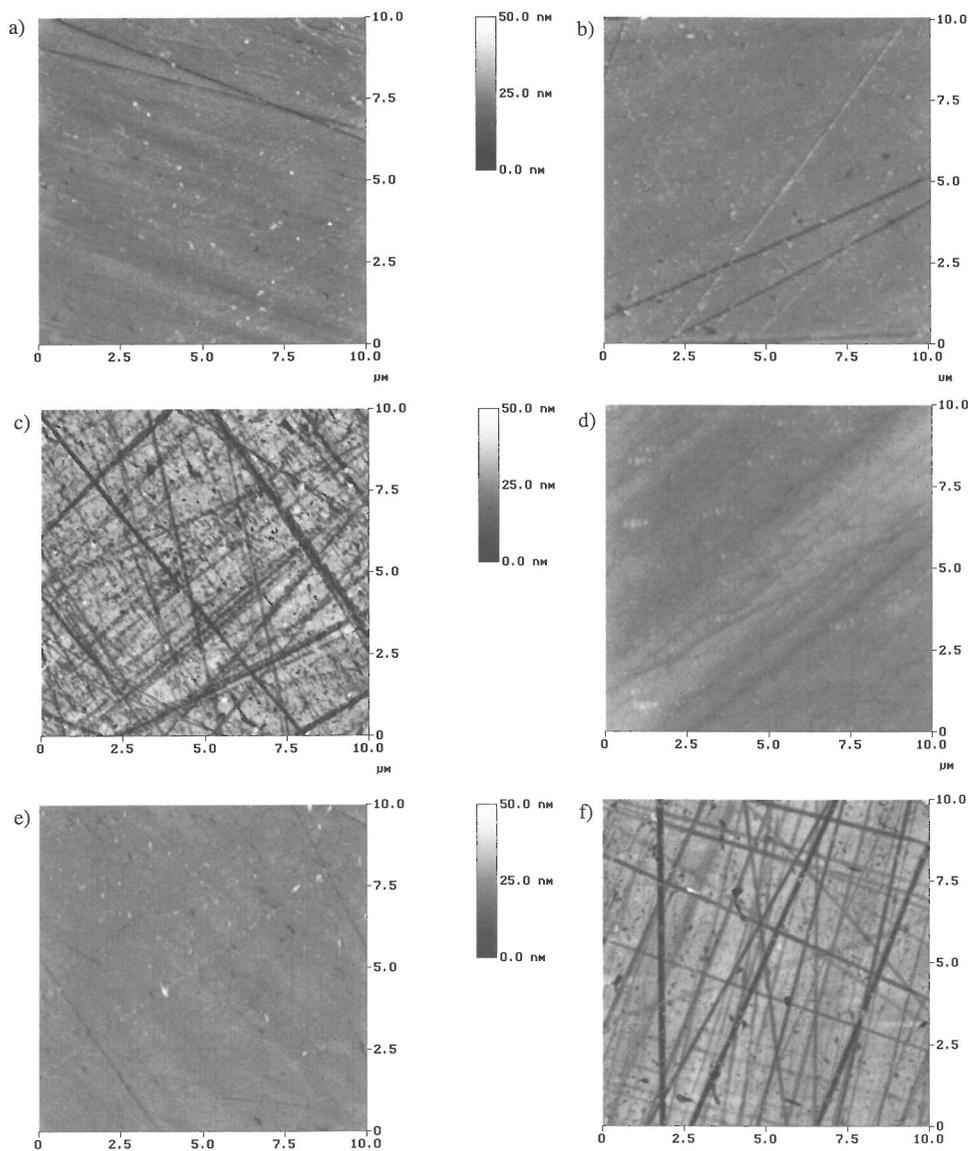
Fig. 1. Atomic force microscope images of polished albite crystal and glass samples showing distribution of surface features: (a) albite crystal unleached, (b) albite glass unleached, (c) albite crystal leached at pH 2 for 5000 h, (d) albite glass leached at pH 2 for 5000 h, (e) albite crystal leached at pH 9 for 5000 h, and (f) albite glass leached at pH 9 for 5000 h. Note the prevalence of polishing lines on most surfaces. All images are 10 μm x 10 μm.

depending upon whether a new or duller tip is used. Except where noted, all roughness values referred to in the text were derived from images of 10 μm x 10 μm areas of the surface.

RMS roughness calculations were performed with Digital Instruments software (Digital Instruments, 1997). Third-order plane fitting was performed on each image prior to analysis to remove any image distortions caused by the curvature of the piezoelectric

material, thermal drift, or lateral forces from sample images (Ruppe and Duparee, 1996). Third-order plane fitting calculates a third-order polynomial fit from the image, removing tilt and S-shaped bow (Digital Instruments, 1997).

Root mean squared roughness (RMS) is defined as the root mean square average of height deviations from the mean elevation plane (standard deviation of the height measurements), calculated from the rela-

tive heights of each pixel in the image:

$$RMS = \sqrt{\left(\left(z_1^2 + z_2^2 + \ldots\ldots + z_N^2 \right) \middle/ N \right)} \quad (1)$$

where z_i equals the difference in height from the mean plane for each point i, and N equals the number of points measured.

Surface area, A, was calculated on three to seven 10 µm x 10 µm scans of each albite glass and crystal plate using a tiling method, wherein the areas of triangles drawn between measured points are summed (Digital Instruments, 1997). Roughness ratio (λ), was calculated for one representative scan so as to be similar to the roughness as defined by Helgeson (1984):

$$\lambda = \left(A \middle/ A_{geo} \right) \quad (2)$$

where A_{geo} is the surface area calculated from the product of the length and width of the scanned field.

Random surface topography can be modeled as a summation of sine waves through two-dimensional Fast Fourier Transform (FFT) analysis; the power spectral density (PSD) function is defined as the square of the FFT (Bennet and Mattson, 1989). Power spectral density (PSD) plots describe the spatial distribution of roughening by plotting the roughness amplitude squared as a function of frequency or wavelength (Digital Instruments, 1997). Power spectra were determined on leached (pH 2.0) and unleached samples as an average over all directions in the data. In contrast to the images used for RMS roughness, the images used for PSD plots were made of different scan areas (1 µm x 1 µm, 5 µm x 5 µm, etc.) representing different resolutions chosen from different places on each sample. Every attempt was made to use images for power spectral determinations which were void of identifiable tip artifacts, noise, and "dust".

3. RESULTS

Unleached albite crystal plates are polycrystalline, and even after polishing, twin planes, cleavage planes, scars from rip-up clasts, and grain boundaries are imaged with DIC microscopy. Albite crystal plates dissolved in all solutions show similar features. In contrast, polished albite glass exhibits no such features under DIC before or after dissolution (DIC images not shown).

Under the AFM, polished, unleached mineral and glass plates show smooth surfaces with few polishing scratches (Figs. 1a, b). The number, width, and depth of pits or scratches all increased with dissolution (Figs. 1c, d, e, and f). In general, crystal plates dissolved at pH 9.0 showed fewer pits or scratches than crystal plates dissolved at pH 2.0 for comparable times. In contrast, glass plates dissolved at pH 9.0 showed more pits or scratches than glass plates dissolved at pH 2.0 for comparable times. Twin boundaries were observed under SEM (Hamilton et al., 2000) and AFM (this study) on crystalline samples leached in pH 9.0 solution for 1000 hours, but not on other samples.

As described previously, topographic data were obtained on 10 µm x 10 µm areas of the surface in order

Table 1. Surface measurements on albite crystal and glass

Sample	pH (± 0.3)	Duration of leaching (h)	RMS roughness[1] (nm)	λ^2	λ^3	H	D[4]	D[5]	A_{BET} (m²/g)[6]
Crystal	--	0	1.23±0.14	1.02	1.006	0.13±0.11	2.87±0.11	2.80±0.08	0.06±0.02
	2.0	1000	7.37±0.24						
	2.0	5000	8.10±0.37	1.03	1.189	0.02±0.07	2.92±0.07	2.29±0.07	0.12±0.04
	9.0	1000	4.47±0.33						
	9.0	5000	1.94±0.04						0.06±0.02
Glass	--	0	2.02±0.19	1.03	1.003	0.18±0.01	2.82±0.01	2.67±0.05	0.04±0.01
	2.0	5000	5.04±0.24	1.02	1.005	0.05±0.06	2.95±0.11	2.74±0.06	1.2±0.4
	9.0	5000	6.31±0.50						0.06±0.02

[1]Calculated as the average for 3-20, 5 µm x 5 µm sub-areas, as described in text.

[2]Calculated using a tiling algorithm (Digital Instruments, 1997).

[3]Calculated on one 10 µm x 10 µm area using the algorithm of Lai and Irene (1999a) and Eqn. 2 in the text.

[4]Calculated using the equation: $D = 3-H$ (Eqn. 4 in text).

[5]Calculated from the slope of the power spectral density plot, as described in the text.

[6]As measured using BET Kr adsorption by Hamilton et al. (2000) on powders dissolved in flow experiments for 3000-5000 h. Final pH of solutions was either pH 2.0 or 8.4 (inlet pH was 2.0 or 9.3, respectively).

to maintain constant resolution. However, sub-areas of these scans were typically analyzed in order to avoid dust and tip artifacts in the larger scans. Even with constant resolution, measured RMS roughness was observed to increase with the size of the sub-area analyzed (Fig. 2a). Above 5 μm x 5 μm, the increase in RMS roughness with sub-area dimension was minimal for both glass and crystal; for this reason, roughness was compared for different samples as measured on 5 μm x 5 μm scans.

In general, RMS roughness was larger on samples after dissolution, but varied depending upon where it was measured on the sample. To compare RMS roughness among samples, a best estimate for RMS roughness for each sample was determined as the mean of RMS roughness calculations from 3 – 20, 5 μm x 5 μm sub-areas, from at least 3 representative 10 μm x 10 μm images of each sample (Table 1). Implicitly, we have assumed that the measured values of RMS roughness for a sample form a normal distribution and that the mean of these measurements is the best estimate of the true RMS roughness. Uncertainties in the determinations of the means for samples (Table 1) represent the standard deviations of the 3 – 20 RMS measurements on all sub-areas divided by the square root of the number of sub-areas.

RMS roughness of unleached glass and crystal plates was 1 – 2 nm (Table 1) and changes during dissolution were on the order of 1 to 8 nm for all samples (Figs. 3a, b). In acidic solutions, the RMS roughness of the crystal plates increased to a greater extent (by a factor of 6.6) than the glass (factor of 2.5) after 5000 hours of dissolution (Fig. 3a, b). In contrast, during dissolution in basic solutions for 5000 h, the glass plate roughened to a greater extent (factor of 3.1) than the crystal (factor of 1.6) after 5000 hours of dissolution (Fig. 3a, b). As a result, RMS roughness is greater on crystalline samples dissolved for 5000 hours at pH 2.0 than pH 9.0, while RMS roughness is greater on glass plates dissolved for 5000 hours at pH 9.0 than 2.0.

For the crystal plates, the RMS roughness increased with dissolution at pH 2.0 up to 1000 h, and then increased or stayed roughly constant to 5000 h. In contrast, the RMS roughness of the crystal plate was lower after dissolution for 5000 h at pH 9.0 than after 1000 h. The crystal plate dissolved for 1000 h at pH 9.0 was also the only sample to show etching of twin boundaries.

Little variation in power spectral density for different images of the same sample at the same scan size was observed (Fig. 4a). Thus, the power spectral density plots showed stationarity at this scale (see Dumas et al., 1993).

To compare 4 samples (crystal and glass, unleached and leached), 5 representative plots, with
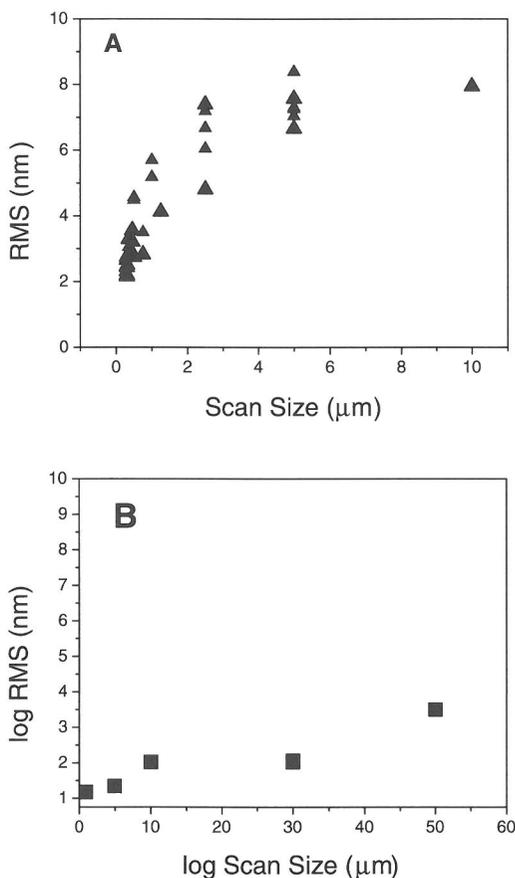

Fig. 2. (a) RMS roughness of albite crystal leached at pH 2 for 1000 h as a function of scan size measured at the same resolution. Each symbol represents a different scan on a different area of the sample. (b) Dependence of RMS roughness on scan size measured at different resolutions on unleached albite glass. A linear relationship implies a self-affine surface

scan dimensions of 1 μm x 1 μm, 5 μm x 5 μm, 10 μm x 10 μm, 30 μm x 30 μm, and 50 μm x 50 μm were analyzed and their power spectra plotted (Figs. 4b, c). For each plot, data for frequencies greater than or equal to the Nyquist frequency for that resolution (0.5 x number of pixels/linear scan dimension) were not used since aliasing can bias the measurement of such signals (Russ, 1994). Unleached glass plates exhibited slightly higher or equal power compared to the unleached crystal plates at all frequencies. For both the crystal and glass plates leached at pH 2.0, increased power with dissolution was observed at all frequencies (Figs. 4b, c); however, the roughness increase at frequencies <10 μm^{-1} was greater for the
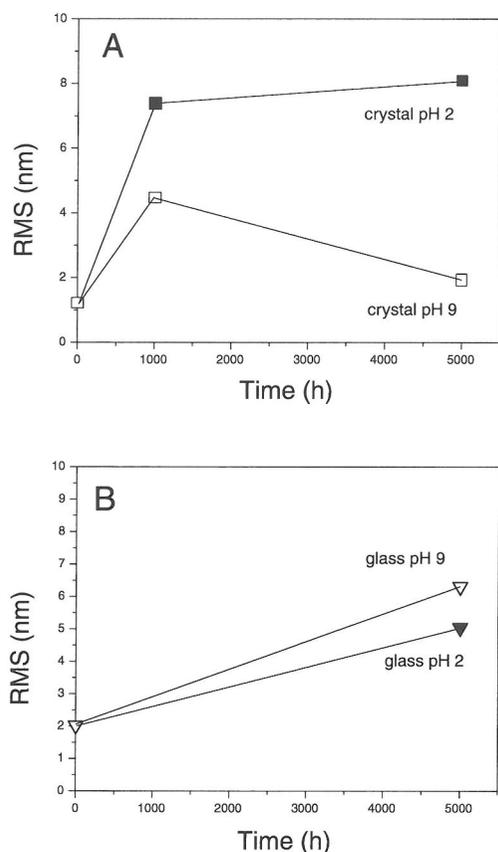
Fig. 3. RMS roughness as a function of dissolution time: (a) albite crystal dissolved at pH 2 (closed squares) and pH 9 (open squares) (b) albite glass at pH 2 (closed triangles) and pH 9 (open triangles).

crystal plates than for the glass plates. RMS roughness determined for each sample (see Fig. 2b for albite glass unleached) for images collected at these five resolutions (1 μm x 1 μm, 5 μm x 5 μm, 10 μm x 10 μm, 30 μm x 30 μm, and 50 μm x 50 μm) increased nonlinearly with scan size.

4. DISCUSSION

4.1. Roughness

Only one sample (albite crystal dissolved at pH 9.0) showed higher roughness after 1000 h than after 5000 h (Fig. 3a). This sample was also the only sample where etched twin boundaries were imaged under AFM. Roughness as measured by AFM for the crystal dissolved at pH 9.0 may therefore have been affected by variability in crystallographic orientation or non-

reproducibilities in surface preparation. If it is assumed that the crystal RMS values at a given pH are the same (within error) after 1000 and 5000 h of dissolution (i.e., assuming that steady-state conditions of dissolution were achieved after 1000 h, see pH 2 results, Fig. 3a), then it is possible that the difference in RMS measured at pH 9 for the crystal (RMS = 4.47 nm after 1000 h, RMS = 1.94 nm after 5000 h, see Table 1) may also simply be due to the variability inherent to crystal orientation and surface preparation. Thus, based on this difference in RMS values, we assume an error of approximately ±2.5 nm with respect to measured values of roughness for all crystal samples. Therefore, based on this estimated error, the difference in RMS of unleached glass and crystal plates (Table 1) is insignificant.

Increased roughness values (compared to unleached samples) for the samples dissolved at pH 2.0 for 5000 h were documented in both RMS roughness values (Table 1) and in increased power at all frequencies in the power spectra (Fig. 4). Simple geometric arguments might suggest that roughness develops on a dissolving surface as a balance between roughening due to pitting, and smoothing due to annihilation of pits through overlapping growth. For example, Affatigato et al. (1996) argued that RMS roughness on polished glass developed due to etching of flaws caused by diamond abrasive particles, but that annihilation of flaws due to lateral growth of these features smoothed the surface. A third process that could smooth surfaces is surface retreat; for a pitted surface in which pits are not deepening as fast as the overall surface is retreating, a smoother surface should develop.

On crystalline surfaces, pits can develop at point, line, and planar defects, as well as on perfect surfaces. Etching of point defects creates pits which disappear with continued etching (e.g., MacInnis and Brantley, 1992). In contrast, etching of line defects continues until the line defect terminates on another linear or planar defect; however, pits develop at dislocations only if the solution concentration is less than the critical concentration (e.g., Brantley et al., 1986). All solutions at pH 2.0 and 9.0 were far from equilibrium (Hamilton et al., 2000), and development of pits at intrinsic and polishing-induced defects on the crystal plates is therefore expected to have been spontaneous. The difference in RMS roughness on crystals dissolved at pH 2.0 and 9.0 therefore probably results from the difference in the *extent* of etching at crystallographic defects rather than differences in the *initiation* of etch pits on the surface. The greater extent of etching is consistent with the faster observed rate of dissolution at pH 2.0 as compared to pH 9.0 (Hamilton et al.,
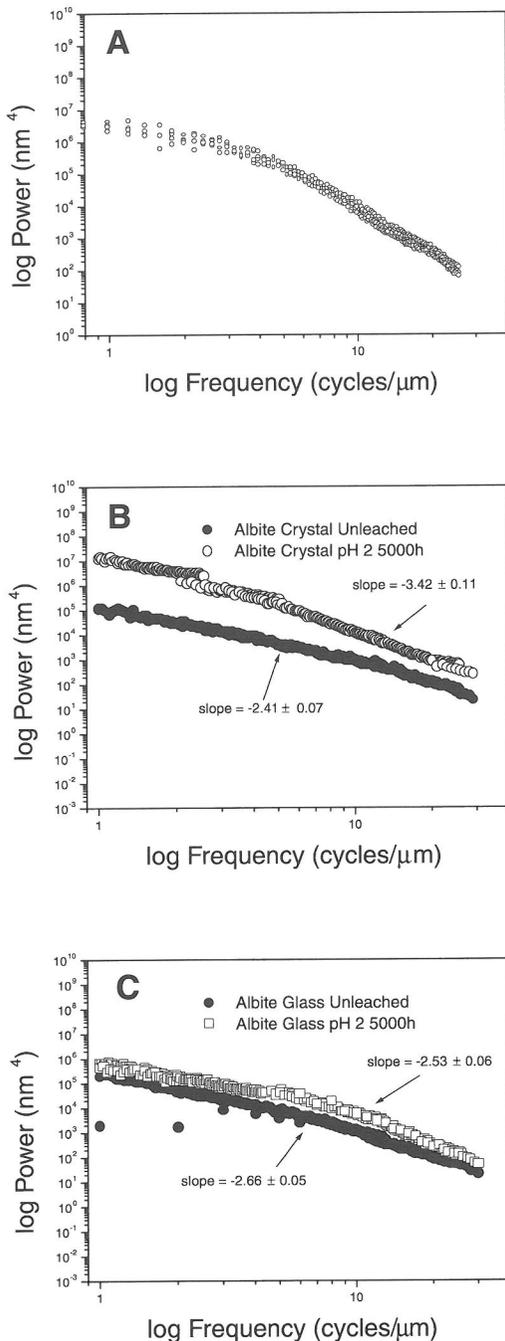
Fig. 4. Characteristic log power vs. log frequency plots of five 10 μm x 10 μm scans from 3 separate spots on (a) an albite crystal leached in a pH 2 solution for 5000 hours. Log power vs. log frequency plots of (b) albite crystal unleached and leached in a pH 2 solution for 5000 h (note: a different spot than shown in part (a)), and (c) glass samples unleached and leached for 5000 h in a pH 2 solution.

2000). However, in relatively strain-free crystals such as the Amelia albite used here, the density of line defects is ~10^6 cm^{-2} (e.g. Casey et al., 1988) and only about 1 defect outcrop per 10 μm x 10 μm image would be expected. Roughness of the surface measured by AFM was therefore most likely related to pitting on perfect surfaces, or at defects induced by polishing. However, variability in crystallographic orientation from one spot to another on the Amelia albite samples makes unambiguous interpretation of roughness impossible for these polycrystalline samples.

The greater roughness on the crystal plates dissolved at pH 2.0 as compared to pH 9.0 might also be hypothesized to be related to nonstoichiometric leaching of the surface (and near surface) and structural changes in that leached (near) surface. Hamilton et al. (2000) reported that at pH 2.0, both Na and Al were significantly depleted in the upper 10 nm of the crystal plate surface after dissolution for a thousand hours. The extent of Na and Al depletion was much smaller at pH 9.0 than at pH 2.0. If RMS roughness correlated with surface leaching, however, then we would have expected a much larger roughness on the acid-dissolved glass plates than was observed, since the upper 10 nm of the albite glass was almost 100% depleted after dissolution at pH 2.0 compared to significantly less depletion after dissolution at pH 9.0 (Hamilton et al., 2000). Despite this enhanced surface leaching at low pH, the glass plates dissolved at pH 9.0 showed the same RMS roughness as the glass plates dissolved at pH 2.0 (Table 1), assuming an uncertainty of ±2.5 nm. Preferential leaching at the surface and near surface apparently does not introduce significant RMS roughness on albite glass or crystal at the scale of measurement of the AFM.

In contrast, adsorption of Kr on the glass powder (Table 1) after 4000 h of dissolution at pH 2.0 documented the development of a leached layer which is porous to gas adsorbate atoms. If the leached layer on the dissolved plate was also porous, the pores that outcropped on the surface were only minimally accessible to the AFM tip or were not present in great abundance. The cross-sectional area of Kr adsorbate gas is 15.2 Å^2 (at 78 K, Gregg and Sing, 1982), while the diameter of the AFM tip is on the order of 10-20 nm.

While the RMS roughness of the crystal plates was larger when dissolved at pH 2.0 than at pH 9.0, the roughness of the glass plate was the same within error (±2.5 nm) after dissolution at these two values of pH. For both crystal and glass powders, the difference in the dissolution rates at pH 8.4 and 2.0 in the flow experiments was approximately an order of magnitude (Hamilton et al., 2000). Affatigato et al. (1996) ob-
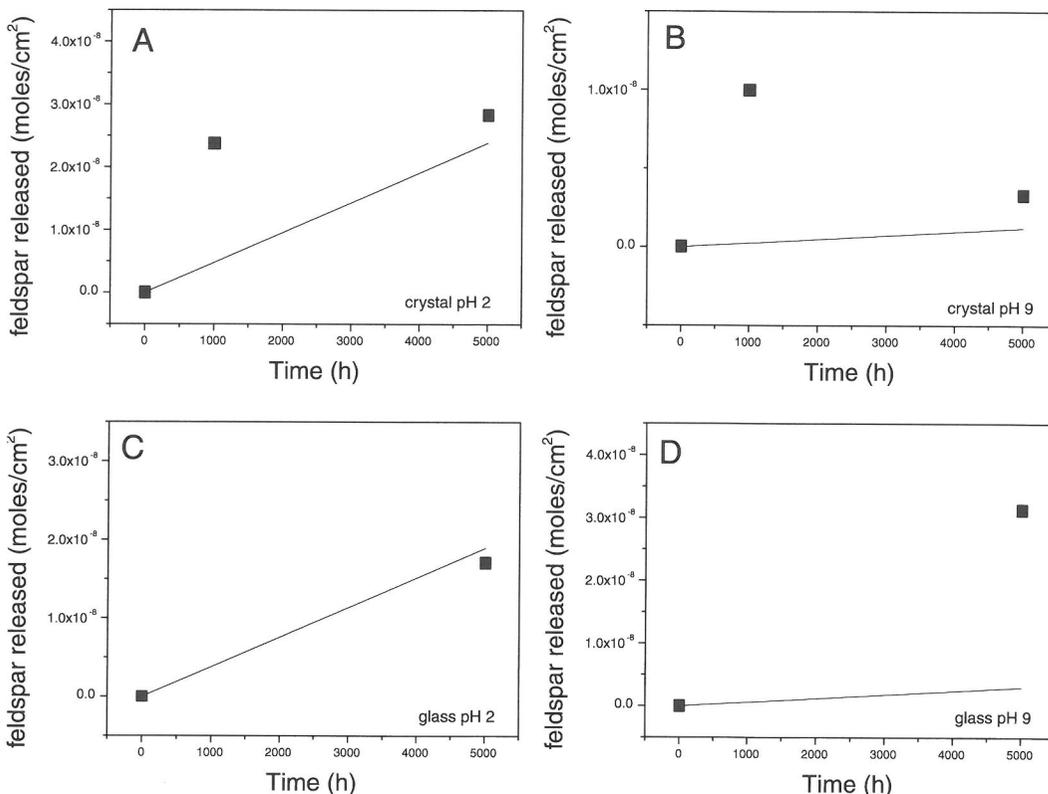
Fig. 5. Moles of released feldspar ($NaAlSi_3O_8$) calculated as a function of time (closed squares) as described in text for A) albite crystal dissolved at pH 2, B) albite crystal dissolved at pH 9, C) albite glass dissolved at pH 2, D) albite glass dissolved at pH 9. Solid line represents expected steady-state release of feldspar as a function of time as calculated from powder dissolution rates from Hamilton et al. (2000) for crystal or glass in flow experiments with outlet values of pH of 2.0 or 8.4 (inlet pH of 2.0 and 9.0, respectively). Moles of feldspar calculated from AFM measurements have been corrected so that the release at time zero equals zero (i.e., calculations were corrected for starting roughness).

served that deepening of initial flaws on silica glass occurred quickly during dissolution, while lateral growth (smoothing) occurred more slowly and became more important in the latter stages of dissolution. It is possible that such smoothing occurred to a greater extent on the acid-dissolved than on the base-dissolved sample, explaining the similarity in roughness of the two samples.

It is also possible that the presence of a leached, porous layer, if it developed on the glass plates, encouraged smoothing instead of roughening. Jordan et al. (1999) observed dissolution of anorthite and labradorite at pH 2.0 with AFM at above ambient temperatures and concluded that dissolution occurred mainly beneath an altered surface layer. They concluded that the topography of the outer surface mim-

icked that of the interface beneath the layer. Similar results were also found in a study of in situ albite dissolution at 25 °C with AFM by Hellmann (1992). If such a dissolving interface exists below a porous surface layer on the albite glass studied here, and if the dissolved concentration of solutes in the pore solutions within the porous layer are higher than in bulk solution, then the surface topography beneath the porous layer might be expected to be smoother than if no layer were present. In other words, within the porous layer, the driving force for dissolution would be lower because of the higher activity of dissolved solutes than at the outer surface–aqueous solution interface, where the activity of dissolved solutes might be relatively lower. With a lower driving force for dissolution, the dissolution would not open up pits on the

surface, but would instead occur equivalently at all surface sites, smoothing the interface. This effect, if important, would be expected to be most important on the glass sample leached at pH 2.0, possibly explaining the relatively smooth surface of that sample.

Removal of complete layers of material (i.e., without roughening) will contribute to dissolution. However, such removal is difficult to quantify by the AFM without a reference for the initial surface height. For our samples, the apparent rate of dissolution was estimated using AFM by calculating the bearing volume. The bearing volume is an estimate of the minimum volume of material removed from the plates (Digital Instruments, 1997); this volume is defined by the difference between a reference plane and the geometric surface area of the sample. The bearing volume was determined for ten to twenty 5 μm x 5 μm scans on at least 4 different images of each crystal and glass sample. Of these measurements, one representative determination of bearing volume was chosen. For this image, the reference plane for the calculation was set as the highest point on the image. The bearing, or "removed" volume, was converted into moles of released feldspar per unit area for each batch experiment using the molar volume of albite crystal or glass. These removed volumes were normalized by the scan area for calculation of dissolution rates. However, Si concentrations in solution as measured by Hamilton et al. (2000) for the plates dissolved here were too low for detection by ICP-AES (<0.1 ppm Si) and solutions were not stored for other types of analysis. For comparison, however, the extent of dissolution of the samples is compared to the measured rates of dissolution on the powders as reported by Hamilton et al. (2000) at steady state for similar values of pH in flow-through reactors (e.g., Fig. 5).

Calculated feldspar released per unit area based on AFM is observed to be always within about an order of magnitude of feldspar released as calculated from solution chemistry. In most cases, the number of moles of feldspar released based on AFM is larger than that based on the powder dissolution experiments (Hamilton et al., 2000). The surprisingly close agreement between rates based on solution chemistry and surface topography may suggest that AFM could be used to measure dissolution rates using this methodology for these phases. Possibly, with these slowly dissolving phases, no overall surface retreat had occurred, even over 5000 h. However, the relative agreement documented by Fig. 5 may also be fortuitous given that the powder dissolution rates were normalized by BET surface area but were extrapolated to this system using the geometric surface area of the AFM scanned image (25 μm^2). The discrepancy between the BET and AFM surface areas for these plates is unknown. The relative agreement exhibited in Fig. 5 suggests, however, that future investigations might eventually yield meaningful dissolution rates based on such AFM measurements, especially if the initial surface height is measured.

4.2. Fractal Dimension

Several authors have pointed out (Varnier et al., 1989; Dumas et al., 1993; Lai and Irene, 1999a) that RMS roughness is only a measure of the vertical component of roughness and does not describe the distribution of topography at the surface. To understand one such measure of the distribution, the fractal dimension, it is helpful to note that RMS roughness of images of the same resolution increased non-linearly with image size (Fig. 2a). Other workers have similarly reported a critical scan dimension above which the change in RMS roughness of a polished surface became minimal with image dimension (e.g. Dumas et al., 1993; Affatigato et al., 1996). By definition, if a surface shows self-affine fractal behavior, the RMS roughness values for the surface should scale as a power law of the image size (Dumas et al., 1993; Gollion and Grenet, 1996):

$$RMS \ \alpha \ L^H \qquad (3)$$

where L is the linear dimension of the scan, and H is a constant known as the scaling factor or roughness index. Gollion and Grenet (1996) point out that L in Eqn. 3 can be varied using AFM by changes in imaged area at one resolution (Fig. 2a) or by a variation in the resolution of images (Fig. 2b). They also point out that the latter method is preferable for calculation of H. The second method, when applied to the unleached albite glass surface (Fig. 2b), yielded $H = 0.18 \pm 0.01$. When applied to a limited data set collected for the three other samples, the linear model could not be rejected, suggesting these four surfaces (surfaces of glass and crystal, unleached and leached for 5000 h) are self-affine (Table 1).

Dumas et al. (1993) showed that this scaling factor H is related to the fractal dimension D:

$$D = 3 - H \qquad (4)$$

Thus, the fractal dimension defines the scaling law relating roughness and sampled area (Fig. 2). Fractal dimensions for rough surfaces are non-integral numbers between 2 and 3, where a value of 2 represents the dimension of a Euclidean plane and 3 an infinitely rough surface (e.g., Dumas et al., 1993; Spanos and Irene, 1994; Lai and Irene, 1999a). Surfaces with low fractal dimension are simpler, with more surface features of low aspect ratio, while surfaces with fractal

dimension near 3 approach volume-filling surfaces, dominated by surface features of high aspect ratio. Spanos and Irene (1994) point out that both the irregularity and the volume-filling nature of a surface increases with increasing D. They also give examples of surfaces with different total roughness that have identical RMS roughness but differing D.

Values of D calculated from Eqn. 4 are identical within error for the unleached glass and crystal plates (Table 1). D increases slightly for the glass plates after dissolution at pH 2.0 (Table 1), while the crystal shows only a slight increase or no change in D with dissolution.

Numerous other methods of quantifying the fractal dimension of a surface are available, and their respective advantages and disadvantages have been investigated (Pfeifer, 1984; Dubuc et al., 1989; Mitchell and Bonnell, 1990). In this study, the 2-D Fast Fourier method is applied (Russ, 1994; Dumas et al., 1993). According to Dumas et al. (1993) and Vatel et al. (1993), when log power is plotted against log frequency for scans of different areas at different resolution, the slope (S_{PSD}) of the line defines D:

$$S_{PSD} = -8 + 2D \tag{5}$$

To estimate D using Eqn. 5, the slope of the power spectral data (Fig. 4) was fit over the entire frequency range, discarding data at < 1 cycle per micron frequency. Furthermore, no data above 30 cycles per micron, where tip dimension would impair resolution, were used. However, because of curvature in the PSDs, several fits were also made, including smaller subsets of the data, to estimate the error associated with truncation of the frequency range. Error estimates for values of D summarized in Table 1 therefore represent variability in the slope as calculated over different ranges of data.

In three of four samples, the value of D calculated from H using Eqn. 4 was close in magnitude to the value calculated from Eqn. 5 (Table 1). Only the crystal plate dissolved at pH 2.0 yielded values of D that differed markedly when calculated with the two equations.

The values of D calculated from Eqn. 5 show that the 2 starting materials have identical D within error and that D may have increased slightly for the glass after dissolution (Table 1). However, D calculated from Eqn. 5 decreased significantly for the crystal plate after dissolution at pH 2.0. Given the curvature in the PSDs, especially for the PSD for the crystal plate dissolved at pH 2.0, estimation of a slope is difficult and this decrease in fractal dimension may not be accurate. Furthermore, this value of D is calculated from data for five different images on the

surface. Given that the surface was polycrystalline, calculation of D may be suspect or meaningless for this sample.

Both calculations of D show that the fractal dimension of the glass plates remains unchanged or increases after dissolution at pH 2.0. This observation can be seen qualitatively in Fig. 4C, based on the similarity in slopes for both glass samples. Henderson et al. (1997) also observed no change in D for glasses after dissolution. Again, assuming that the fractal dimension of a porous surface layer should be significantly closer to 3 than D for the polished surface, we infer that the AFM is not measuring the internal surface area of such a layer on the acid-dissolved glass sample, as expected based on the geometry of measurement by an AFM tip. Hamilton et al. (2000) concluded from XPS and SIMS data that the thickness of the leached layer was in the range 9 - 50 nm on glass plates leached at pH 2.0.

4.3. Increases in Surface Area

Although RMS roughness increased with dissolution for all samples, λ, the ratio of measured surface area to geometric surface area (see Eqn. 2), calculated using a tiling algorithm (Digital Instruments, 1997; see also, discussion in Brantley et al., 1999), increased for the crystal plate but decreased for the glass plate after dissolution (Table 1). This observation is puzzling since measured BET surface areas increased for all samples after dissolution (Table 1). However, Lai and Irene (1999a) have suggested that the tiling method may underestimate surface area for surfaces with RMS roughness values such as those reported here (Table 1), where the magnitude of deviations in the z direction (vertical) are much less than the horizontal resolution. The algorithm for calculation of surface area by tiling is neither accurate nor sensitive due to round-off error (Lai and Irene, 1999a). These workers suggest an alternative algorithm to calculate surface area, $A_{(rms, D_f)}$, using AFM data:

$$A_{(rms, D_f)} = \left(a' \, RMS \, e^{bD} \right)^2 \tag{6}$$

where a' and b are weighting factors dependent upon scan dimensions, D is the fractal dimension, and RMS is RMS roughness. This equation should yield a more accurate estimation of surface area for samples with microscopic roughness such as those in this study (Lai and Irene, 1999a), as compared to the tiling calculation (Digital Instruments, 1997). Using Eqn. 6, Lai and Irene (1999a) have shown that two surfaces with identical RMS roughness can differ in surface area and total roughness, due to the spatial distribution of roughness

(fractal dimension). The authors show that for surfaces with identical RMS roughness, the area increases as fractal dimension increases (Lai and Irene, 1999b).

Using the Lai and Irene algorithm (1999a), and calculating values for a' and b according to the empirical methods outlined in Lai and Irene (1999a), the surface area was calculated based upon D and RMS roughness measured on one 10 μm x 10 μm area on both glass and crystal plates. For both cases surface area increased with dissolution, albeit by a small fraction (Table 1). In contrast to the BET data for similarly dissolved powder, however, the surface area of the crystal increased more drastically than the surface area of the glass (Table 1). Again, this re-emphasizes that BET measures the outer surface and some part of the porous leached layer internal near surface, whereas the AFM only measures some part of the outer surface.

Mineral dissolution rates are almost always cited as moles of phase "x" released per unit time per unit surface area (as measured by BET), even though many workers have suggested that the *reactive* surface area might differ from the BET measured area (see Brantley and Mellott, 2000 for a review). However, Hamilton et al. (2000) point out that Si release rates of albite glass did not increase during dissolution even while surface area increased by a factor of 30x. Casey et al. (1989) made similar conclusions based on observations of increased surface area without an increase in dissolution rate for labradorite feldspar. The main arguments for normalization of most mineral dissolution rates by BET surface area of the mineral instead of reactive surface area are: i) there is no agreement about how to assess reactive surface area, and ii) reactive surface area is assumed to be proportional to BET surface area. Apparently, the ratio of reactive/total (BET) surface area for the albite glass changed during dissolution at low pH. Other authors have observed similar phenomena for naturally weathered phases (Lee and Parsons, 1995). One positive attribute of the AFM measurement of surface area is that this surface area remained relatively constant during dissolution of the albite glass plate at pH 2.0, instead of increasing drastically, as was observed for the BET surface area of the albite glass powder. Brantley et al. (1999) discussed the difference between surface area measured using BET and using AFM on naturally etched quartz grains and pointed out that little is known about the topographic features that are measured by both tools. Further assessment of surface area algorithms and measurements of roughness (e.g., RMS, power spectral density, correlation lengths) based on AFM measurements may be useful in clarifying the notion of *reactive* surface area.

5. CONCLUSIONS

Atomic force microscopy (AFM) of polished surfaces of glass and crystal of albite composition were analyzed before and after dissolution at pH 2.0 and 9.0. The roughness of the crystal plates dissolved at pH 2.0 was larger than the same phase dissolved at pH 9.0. Enhanced RMS roughness on the dissolved crystal plates at pH 2.0 is interpreted as evidence of the greater extent of etching at defects at the lower pH, consistent with faster dissolution at lower pH. In contrast, the RMS roughness of glass plates dissolved at pH 2.0 was identical within error to that phase dissolved at pH 9.0, despite faster dissolution at low pH. The difference in roughness developed on crystal and glass plates cannot be explained unambiguously given the polycrystallinity of the crystal plates and the possibility of variations in polishing effects. However, AFM did not document large increases in RMS roughness due to nonstoichiometric dissolution in either crystal or glass.

Total roughness of the surfaces could not be measured without measuring the spatial distribution (fractal dimension D) as well as the vertical component of roughness (RMS). RMS roughness and fractal dimension were used to calculate surface area of plates dissolved at pH 2.0. The surface area measured by the AFM at this scale increased only slightly over 5000 h of dissolution at pH 2.0 for both phases. In contrast, the BET surface area of glass powder dissolved at pH 2.0 showed a 30-fold increase in BET surface area after 4000 h dissolution, despite the observation that the Si release rate of the glass showed no significant increase with extent of dissolution. Feldspar dissolution rates calculated from AFM measurements were within a factor of 10 of inferred dissolution rates, even though no attempt was made to measure the initial surface height nor the rate of surface retreat by removal of entire atomic layers. If results from polished samples can be extrapolated to powders, then the AFM-measured surface area may be a better proxy for reactive surface area on albite samples than BET surface area. Significant problems remain, however, in calculating surface area from AFM measurements for polished samples or powders. Additional research should focus on comparing solution measurements with AFM measurements of topography including RMS roughness, correlation length, and power spectral density.

REFERENCES

Affatigato M., Osborne D.H., and Haglund R.F. (1996) Changes in the surface morphology of glass due to abrasion and the deposition of sol-gel thin films. *J. Non-Crys. Solids* **181**, 27-38.

Anbeek C. (1992) The dependence of dissolution rates on grain size for some fresh and weathered feldspars. *Geochim. Cosmochim. Acta* **56**, 3957-3970.

Bennet J.M. and Mattson L. (1989) *Surface Roughness and Scattering*. Optical Society of America Publication.

Blum A.E., Yund R.A., and Lasaga A.C. (1990) The effect of dislocation density on the dissolution rate of quartz. *Geochim. Cosmochim. Acta* **54**, 283-297.

Brantley S.L., Crane S.R., Crerar D.A., Hellmann R., and Stallard R. (1986) Dissolution at dislocation etch pits in quartz. *Geochim. Cosmochim. Acta* **50**, 2349-2361.

Brantley S.L., White A.F., and Hodson M.E. (1999) Surface area of primary silicate minerals. In *Growth and Dissolution in Geosystems* (eds. B. Jamtveit and P. Meakin). Kluwer Academic Publishers, Dordrecht. pp. 291-326.

Brantley S.L. and Mellott N.P. (2000) Surface area and porosity of primary silicate minerals. *Amer. Mineral.* **85**, 1767-1783.

Brunauer S., Emmett P.H., and Teller E. (1938) Adsorption of gases in multimolecular layers. *J. Am. Chem. Soc.* **60**, 309-319.

Casey W. H. and Bunker B. (1990) Leaching of mineral and glass surfaces during dissolution. In *Mineral-Water Interface Geochemistry* (eds. M. F. Hochella Jr. and A. F. White). Reviews in Mineralogy, Vol. 23, Mineralogical Society of America, Washington, D.C. pp. 397-425.

Casey W.H., Carr M.J., and Graham R.A. (1988) Crystal defects and dissolution kinetics of rutile. *Geochim. Cosmochim. Acta* **52**, 1545-1556.

Casey W.H., Westrich H.R., Massis T., Banfield J.F., and Arnold, G.W. (1989) The surface of labradorite after acid hydrolysis. *Chem. Geology* **78**, 205-218.

Digital Instruments (1997) *Nanoscope Command Reference Manual*, V. 4.31, Rev. B.

Dubuc B., Zucker S.W., Tricot C., Quiniou J.F., and Wehbi D. (1989) Evaluating the fractal dimension of surfaces. *Proc. R. Soc. London, Ser A* **370**, 113-127.

Dumas P.H., Bouffakhreddine B., Amra C., Vatel O., Andre E., Galindo R., and Salvan F. (1993) Quantitative microroughness analysis down to the nanometer scale. *Europhys. Lett.* **22**, 717-722.

Fenter P., Teng H., Geissbühler P., Hanchar J.M., Nagy K.L., and Sturchio N.C. (2000) Atomic-scale structure of the orthoclase (001)-water interface measured with high-resolution x-ray reflectivity. *Geochim. Cosmochim. Acta* **64**, 3663-3673.

Gollion P. and Grenet G. (1996) Determination of fractured steel surface roughness by atomic force microscopy using fractal-based approaches. *Surface Interface Anal.* **24**, 282-285.

Gregg S.J. and Sing K.S.W. (1982) *Adsorption, Surface Area and Porosity*. Academic Press, London.

Hamilton J.P., Pantano C.G., and Brantley S.L. (2000) A comparison of the dissolution and leaching behavior of albite crystal and glass in acidic, neutral, and basic conditions. *Geochim. Cosmochim. Acta.* **64**, 2603-2616.

Helgeson H.C., Murphy W.M., and Aagaard, P. (1984) Thermodynamic and kinetic constraints on reaction rates among minerals and aqueous solutions II. Rate constants, effective surface area, and the hydrolysis of feldspar. *Geochim. Cosmochim. Acta* **48**, 2405-2432.

Hellmann R. (1995) The albite-water system: Part II. The time-evolution of the stoichiometry of dissolution as a function of pH at 100, 200, and 300 °C. *Geochim. Cosmochim. Acta* **59**, 1669-1697.

Hellmann R. (1997) The albite-water system: Part IV. Diffusion modeling of leached and hydrogen-enriched layers. *Geochim. Cosmochim. Acta* **61**, 1595-1611.

Hellmann R., Drake B., and Kjoller K. (1992) Using atomic force microscopy to study the structure, topography and dissolution of albite surfaces. In *Water-Rock Interaction 7*, Vol. I (eds. Y. K. Kharaka and A. S. Maest). A.A. Balkema, Rotterdam. pp. 149-152.

Henderson S., Castle J., and Zhdan P. (1997) The SPM and XPS characterization of the corrosion resistance of glasses. In *Advances in the Characterization of Ceramics* (eds. R. Freer, B. Derby, and B.H. Lewis). British Ceramics Proc., pp. 54-66.

Jordan G., Higgins S.R., Eggleston C.M., Swapp S.M, Janney D.E., and Knauss K.G. (1999) Acidic dissolution of plagioclase: In-situ observations by hydrothermal atomic force microscopy. *Geochim. Cosmochim. Acta* **63**, 3183-3193.

Lai L. and Irene E.A. (1999a) Area evaluation of microscopically rough surfaces. *J. Vac. Soc. Tech. B* **17**, 33-39.

Lai L. and Irene E.A. (1999b) Limiting Si/SiO$_2$ interface roughness resulting from thermal oxidation. *J. App. Phys.* **86**, 1729-1739.

Lasaga A.C. and Blum A.E. (1986) Surface chemistry, etch pits and mineral-water reactions. *Geochim. Cosmochim. Acta* **50**, 2363-2379.

Lee M.R. and Parsons I. (1995) Microtextural controls of weathering of perthitic alkali feldspars. *Geochim. Cosmochim. Acta* **59**, 4465 - 4488.

Lee M.R., Hodson M.E., and Parsons I. (1998) The role of intragranular microtextures and microstructures in chemical and mechanical weathering: direct comparisons of experimentally and naturally weathered alkali feldspars. *Geochim. Cosmochim. Acta* **62**, 2771-2788.

MacInnis I.N. and Brantley S.L. (1992) The role of dislocations and surface morphology in calcite dissolution. *Geochim. Cosmochim. Acta* **56**, 1113-1126.

Mitchell M.W. and Bonnell D.A. (1990) Quantitative topographic analysis of fractal surfaces by scanning tunneling microscopy. *J. Mat. Res.* **5, 10**, 2244-2254.

Pfeifer P. (1984) Fractal dimension as a working tool for surface-roughness. *Applic. Surface Sci.* **18**, 146-164.

Ruppe C. and Duparee A. (1996) Roughness analysis of optical films and substrates by atomic force microscopy. *Thin Solid Films* **288**, 8-13.

Russ J. (1994) *Fractal Surfaces*. Plenum Press, New York.

Spanos L. and Irene E.A. (1994) Investigation of roughened silicon surfaces using fractal analysis I. Two-dimensional variation method. *J. Vac. Soc. Tech. A* **12**, 2646-2652.

Stillings L.L. and Brantley S.L. (1995) Feldspar dissolution at 25 °C and pH 3: Reaction stoichiometry and the effect of cations. *Geochim. Cosmochim. Acta* **59**, 1483-1496.

Varnier F., Mayani N., and Rasigni G. (1989) Surface roughness and the fractal nature of thin films of MgF_2 and Ag/MgF_2. *J. Vac. Sci. Technol. A* **4**, 1289-1293

Vatel O., Dumas P., Chollet F., Salvan F., and Andre E. (1993) Roughness assessment of polysilicaon using power spectral density. *J. App. Phys.* **32**, 4921-4922.

White A.F. and Peterson M.L. (1990) Role of reactive-surface-area characterization in geochemical kinetic models. In *Chemical Modeling of Aqueous Systems II.* Amer. Chem. Soc. Symp. Ser. 416, American Chemical Society, Washington, D.C. pp. 461-475.

Zellmer L.A. (1986) Dissolution kinetics of crystalline and amorphous albite. M. Sc. thesis, The Pennsylvania State University, University Park, PA (USA).